Journal of Engineering Science *Vol. XXIX, no. 1 (2022), pp. 71 - 85*
Fascicle *Electronics and Computer Science* *ISSN 2587-3474*
Topic *Electronics and Communication* *eISSN 2587-3482*

https://doi.org/10.52326/jes.utm.2022.29(1).06
CZU 623.4.021:004.6

SYSTEMS FOR INVARIANT TARGET RECOGNITION BASED ON CENTRAL IMAGE CHORD TRANSFORMATION

Veaceslav Perju*, ORCID 0000-0002-7755-4277

Department of Strategical Studies in Defense and Security
Agency for Military Science and Memory
47 Tighina Str., Chisinau, MD-2001, Republic of Moldova
*Corresponding author: Veaceslav Perju, *vlperju@yahoo.com*

Received: 12.10.2021
Accepted: 02.06.2022

Abstract. Target recognition (TR) is widely used in different military and civil applications and permits enhanced intelligence and autonomously operating platforms design. The article describes existing systems for TR such as deep learning aided computer vision; target tracking architecture, based on the tracking-by-detection paradigm; a target detection dataset; deep neural networks; a system for the management of a plurality of sensors; a target recognition architecture, adaptive to operational conditions and a target detection system, based on the theory of multi-temporal recognition. Unfortunately, the existing systems do not orient for real-time processing or can be applied for synthetic aperture radar images only, or used for image processing of soft targets, etc. This article presents the data regarding proposed new systems for targets recognition and determination of their parameters, based on central image chord transformation. The systems' main processing units are described. The structures of the elaborated systems and the principles of their functioning are presented. The models of data processing flow in the systems are described. The determination of the processing time of the operations, realized in the systems was made and the estimation of the throughput of the systems was done. The optimization of the elaborated systems was made. The results regarding systems' characteristics are presented.

Kew words: *Target recognition, data processing flow, throughput, optimization.*

Rezumat. Recunoașterea țintei (RȚ) este utilizată pe scară largă în diferite aplicații militare și civile și permite proiectarea platformelor de operare autonomă inteligente îmbunătățite. Articolul descrie sisteme existente pentru RȚ, cum ar fi vizualizarea computerizată asistată de învățare profundă; arhitectura de urmărire a țintei, bazată pe paradigma detecției; utilizarea unui set de date de detectare a țintei; rețele neuronale profunde; un sistemul bazat utilizarea multitudinii de senzori; o arhitectură de recunoaștere a țintei, adaptabilă la condițiile operaționale și un sistem de detectare a țintei, bazat pe teoria recunoașterii multi-temporale. A fost stabilit, că sistemele existente nu permit procesarea datelor în timp real sau pot fi aplicate doar pentru imagini radar sintetice sau utilizate pentru procesarea imaginilor țintelor variabile etc. În acest articol se descriu noile sisteme propuse pentru recunoașterea țintelor și determinarea parametrilor lor, bazate pe transformarea centrală a

coardelor de imagine. Sunt descrise principalele unități de procesare ale sistemelor. A fost prezentate structurile sistemelor elaborate și principiile de funcționare a acestora. Se descriu modelele fluxului de procesare a datelor în sisteme. A fost estimat timpul de procesare a operațiilor, realizate în sisteme și s-a făcut analiza productivității sistemelor. S-a realizat optimizarea sistemelor elaborate. Sunt prezentate rezultatele privind caracteristicile sistemelor.

Cuvinte cheie: *Recunoașterea țintei, flux de procesare a datelor, productivitate, optimizare.*

Introduction

Target recognition is one of the core processes for enhancing intelligence and autonomously operating platforms. Deep learning-aided computer vision systems have yielded promised results on target recognition applications [1]. However, these approaches do not translate easily to engineered realizations. The article [2] presents a target tracking system aimed to be used in real-time conditions. The problems appear in the presents of specific challenges such as moving sensors, changing zoom levels, dynamic background, illumination changes, obscurations, and small objects.

The paper [3] presents a target detection dataset that depicts helicopters. Unfortunately, the targets are seen by the camera in real-world scenarios typically do not always appear large, focused, or in the center of the input image.

The perspective approach for target recognition consists using of deep neural networks [4]. However, within the real conditions appear necessary to define a large number and types of targets' classes. The paper [5] presents a system for the management of a set of sensors to improve the threat-detection capabilities of targets. The system architecture consists of three main components, such as 2D video tracking and re-identification, which allows the labeling and tracking of targets in a small area; 3D video tracking with a stereo camera, which gives a more accurate location measurement using recurrent neural networks for location prediction, and, finally, command and control unit. The data fusion combines the outputs of multiple sensors. Unfortunately, this system can be applied for image processing of the soft targets only.

In the paper [6] an automatic target recognition architecture is proposed, based on the current methodology trends. Unfortunately, the proposed architecture can be applied for synthetic aperture radar images only.

Based on the theory of multi-temporal recognition, an automatic target recognition system for the remote sensing image is proposed in the article [7], which includes four modules: remote sensing image segmentation; target extraction from an image; the processing of the target's image, and recognition of the target. Unfortunately, the elaborated system doesn't orient for real-time processing.

In this article, the systems for invariant target recognition and determination of their parameters – scale, angular rotation, and position in the plane are described, based on the methods of target recognition, proposed by the author in [8]. The elaborated systems are referred to as a specialized multiprocessor functional distributed class of systems, which represent a combination of the electronic and optical processing modules.

In section 1 the systems' main processing units are described. In sections 2 - 5 the structures of the elaborated systems are presented and the principles of their functioning are described. The data processing flow models in the proposed systems are presented in section 6. In section 7 the determination of the processing time of the operations, realized in the systems

was made and the estimation of the data processing time and throughput of the systems are presented. Based on the obtained results the optimization of the elaborated systems was made. The results regarding systems' characteristics are described.

1. The systems' main processing units

Suppose the target is describing as:

$$P'(x',y') = P'(x,y,e_1,e_2, e_3, e_4)=P'(x+e_3,y+e_4,e_1,e_2), \quad (1)$$

were e_1 is scale change, e_2 – rotation, and e_3, e_4 – shits of the target.

The systems described below consist of the next main units: laser (L) as a source of coherent light for data transmission and processing; preprocessing module (PPM) for target's image input and enhancement such as noise-reducing, contrast increasing, etc. [9]; optical multiplier (OM) for light beam dividing (multiplexing); a processor for determining the target's parameters e_3, e_4 (PTP) [10]; a processor for target's scale and rotation (PTSR) determination (parameters e_1, e_2) [11]; a processor for coordinate transformation (PCT) of the target's image [12]; processor for central image chord transformation (PICT) realization [13]; a processor for Fourier transformation (PFT) and determination the target's image complexity SL and maximum frequency f_m of the spectrum [14]; a processor for target's rotation (PTR) determination (parameter e_2) [15]; a processor for system's control, processing of the data and target classification (PCPC) [16].

2. Target recognition system TRS1

The system TRS1 realizes the method TRM1 of the target recognition, proposed by the author and described in [8], and is presented in Figure 1. The system works in the next mode. The target's image P'(x',y') is scanned into the processor PTIP where the operations are realized of the enhancement, noise extraction, etc.

$$P'(x',y') \longrightarrow P(x',y') = P(x,y,e_1,e_2,e_3,e_4). \quad (2)$$

The laser L light beam is modulated by the function P(x',y') in the processor PTIP and at the output is divided by multiplier OM1 into three light beams, which are introduced into the processors PTP, PCT1, and PFT, respectively. In the processor PTP the target's parameters e_3 and e_4 are calculated. In parallel, the Fourier spectrum of the function P(x',y') is formed in the processor PFT:

$$P(x',y') \longrightarrow |FT\{P(x',y')\}|^2=P(x'_1,y'_1) = P(x_1,y_1,e_1,e_2). \quad (3)$$

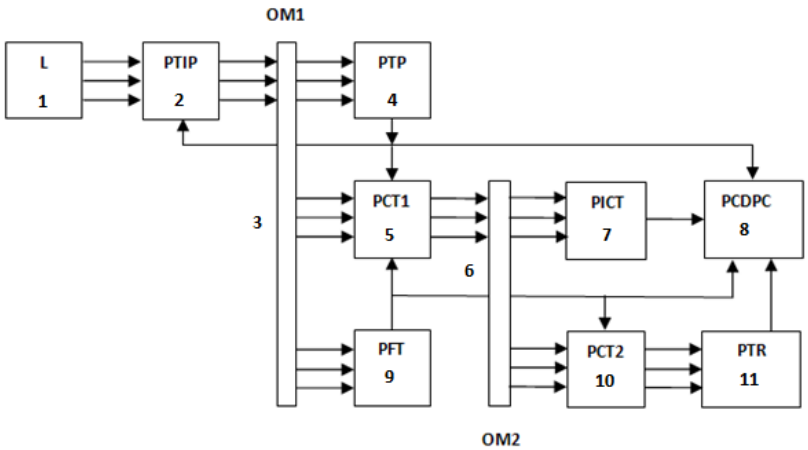

Figure 1. The structure of the system TRS1.

The maximum frequency f_m of the Fourier spectrum $P(x'_1,y'_1)$ and the complexity SL of image P(x',y') are calculated in this processor. The data regarding the target's shifts e_3 and e_4 from processor PTP, and the target's complexity SL from processor PFT are introduced into processors PCT1, about parameter SL – into processor PCT2, and regarding the parameters e_3, e_4, and f_m - into processor PCDPC. In the processor PCT1, the function P(x',y') is centered under parameters e_3, e_4, and SL:

$$P(x',y')=P(x+e_3,y+e_4,e_1,e_2)\rightarrow P(x'_2,y'_2)=P(x_2,y_2,e_1,e_2), \quad (4)$$

where $x_2=x-e_3$, $y_2=y-e_4$.

Then, the function $P(x_2',y_2')$ from the processor PCT1 is input via multiplier OM2 into processors PICT and PCT2. In the processor PICT the chords transformation of the function $P(x'_2,y'_2)$ is realized [13]:

$$P(x'_2,y'_2)\rightarrow P(x'_3,y'_3), \quad (5)$$

and the target's feature vector **v** is calculated. The information regarding vector **v is** sent to the processor PCDPC, where the target is classified [16]. The target's scale e_1 is calculated using the expression $e_1=f_{ms}/f_m$, where f_{ms} is the Fourier spectrum maximum frequency of the reference target.

In the processor PCT2, the function $P(x'_2,y'_2)$ is normalized on the parameter e_1 and is transformed to the polar coordinate system:

$$P(x'_2,y'_2)=P(x_2,y_2,e_1,e_2)\rightarrow P(x'_4,y'_4)=P[x_4+x_{40}(e_2),y_4], \quad (6)$$

where $x'_4=\text{arctg}(y_2/x_2)$, $y'_4=[(x^2_2+y^2_2)^{1/2}]/e_1$.

The function $P(x'_4,y'_4)$ is transmitted from the processor PCT2 to the processor PTR, where the target's scale e_2 is determined at the extraction and processing of the value $x_{40}(e_2)$.

3. Target recognition system TRS2

The system TRS2 realizes the target recognition method TRM2 [8], and the structure is the same as TRS1 (Figure 1). The difference consists in the computer processes organization. The system work in the next mode. The target's image P'(x',y') is introduced into the processor PTIP where the operations are realized of the image enhancement:

$$P'(x',y') \longrightarrow P(x',y')= P(x,y,e_1,e_2,e_3,e_4). \quad (7)$$

The laser L light beam in the processor PTIP scans the image P(x',y'), which is reflected in continuation by multiplier OM1 at the inputs of the processors PTP, PCT1, and PFT. In the processor PTP the target's coordinates e_3 and e_4 are calculated. Simultaneously, the function P(x',y') Fourier spectrum is calculated in the processor PFT:

$$P(x',y') \longrightarrow |FT\{P(x',y')\}|^2=P(x'_1,y'_1) = P(x_1,y_1,e_1,e_2). \quad (8)$$

Based on $P(x'_1,y'_1)$, the complexity SL of image P(x',y') is calculated. The information regarding coordinates e_3 and e_4 from processor PTP, and target's complexity SL from processor PFT is transmitted to processor PCT1, about SL – to processor PCT2, and about e_3 and e_4 - to processor PCDPC. In the processor PCT1, the function P(x',y') is centered following data e_3, e_4, and SL:

$$P(x',y')=P(x+e_3,y+e_4,e_1,e_2)\rightarrow P(x'_2,y'_2)=P(x_2,y_2,e_1,e_2), \quad (9)$$

where $x_2=x-e_3$, $y_2=y-e_4$.

After that, the image $P(x_2',y_2')$ is introduced, via multiplier OM2, into processors PICT and PCT2. In the processor PICT the operation of chord transformation is performed [13]:

$$P(x'_2,y'_2)\rightarrow P(x'_3,y'_3), \tag{10}$$

and a vector **v** of the target's features is calculated. The information from the processor PICT is transmitted to the processor PCDPC, where the operation of target classification is realized [16]. In processor PCT2, the function $P(x'_2,y'_2)$ is transformed to the log-polar coordinate system:

$$P(x'_2,y'_2) = P(x_2,y_2,e_1,e_2) \rightarrow P(x'_4,y'_4)= P[x_4+x_{40}(e_1), y_4+y_{40}(e_2)], \tag{11}$$

where $x_4=\text{arctg}(y_2/x_2)$, $y_4=(x_2^2+y_2^2)^{1/2}$, and $x_{40}(e_1)$, $y_{40}(e_2)$ are the parameters, depending on the values of e_1 and e_2 respectively. In this case, the effects of the target scaling on value e_1 and rotation on value e_2 will produce the shifts of the function $P(x'_4,y'_4)$ on the axis x_4 and y_4 respectively. The function $P(x'_4,y'_4)$ is transmitted from processor PCT2 to processor PTSR, where the parameters value e_1 and e_2 are determined based on the correlation function, calculated between this function and reference target's function $P_s(x_4,y_4)$ determined on the stage of classification:

$$U(x,y) = \max\{\iint P(x'_4,y'_4)P_s(x_4,y_4)\, dx_4dy_4. \tag{12}$$

4. Target recognition system TRS3

The system TRS3 realizes the method TRM3 of the target recognition [8] and is presented in Figure 2.

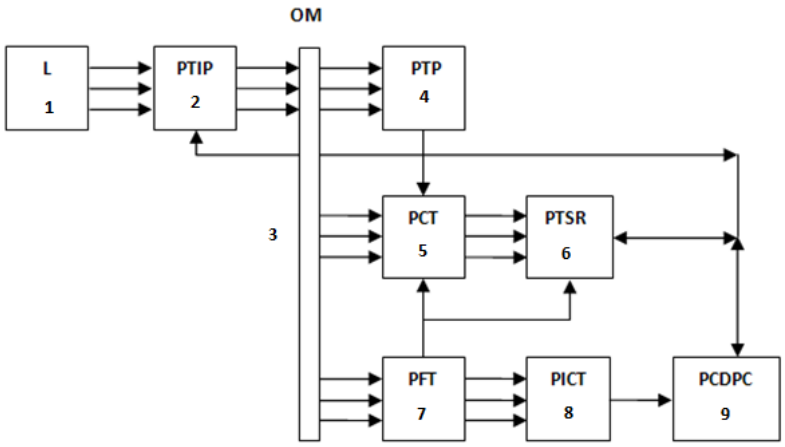

Figure 2. The structure of the system TRS3.

The system operates in the following way. The target's image P'(x',y') is scanned into processor PTIP were are realized the operations of enhancement:

$$P'(x',y') \rightarrow P(x',y') = P(x,y,e_1,e_2,e_3,e_4). \tag{13}$$

The light beam generated by laser L going via processor PTIP is modulated by image P(x',y') after which is introduced via multiplier OM in the processors PTP, PCT, and PFT. In the processor PTP, the target's coordinates e_3, e_4 in the plane are calculated. Contemporaneously, the Fourier spectrum of the input function is calculated in the unit PFT:

$$P(x',y') = P(x,y,e_1,e_2,e_3,e_4) \rightarrow |FT\{P(x',y')\}|^2=P(x'_1,y'_1) = P(x_1,y_1,e_1,e_2). \tag{14}$$

The parameter SL of the function P(x',y') also is determined in this unit. The image $P(x'_1,y'_1)$ is transmitted from processor PFT to the processor PICT, where the operation of chords transformation is performed [13]:

$$P(x'_1,y'_1) \rightarrow P(x'_2,y'_2), \tag{15}$$

Based on this the target's feature vector **v** is calculated. The information regarding vector **v** is transferred from processor PICT to processor PCDPC, where the target is classified [16]. The data about coordinates e_3 and e_4 from processor PTP, and complexity SL - from processor PFT have been introduced into processors PCT, where the function P(x',y') is centered on the parameters e_3, e_4 and is transformed to the log-polar coordinate system:

$$P(x',y')=P(x+e_3,y+e_4,e_1,e_2) \rightarrow P(x'_3,y'_3)=P[x_3+x_{30}(e_2),y_3+y_{30}(e_1)], \tag{16}$$

where $x'_3=\text{arctg}(y''/x'')$, $y'_3=\ln[(x'')^2+(y'')^2]/2$ and $x''=x'-e_3$, $y''=y'-e_4$.

Then, in the processor PTSR the parameters value e_1 and e_2 are determined based on the correlation function calculated between the function $P(x'_3,y'_3)$ and the standard target's function $P_s(x_3,y_3)$ determined on the stage of classification:

$$U(x_4,y_4) = \max\{\iint P(x'_3,y'_3)P_s(x_3,y_3)\, dx_3dy_3\}. \tag{17}$$

5. Target recognition system TRS4

The system TRS4 realizes the method TRM4 of the target recognition [8] and is presented in Figure 3.

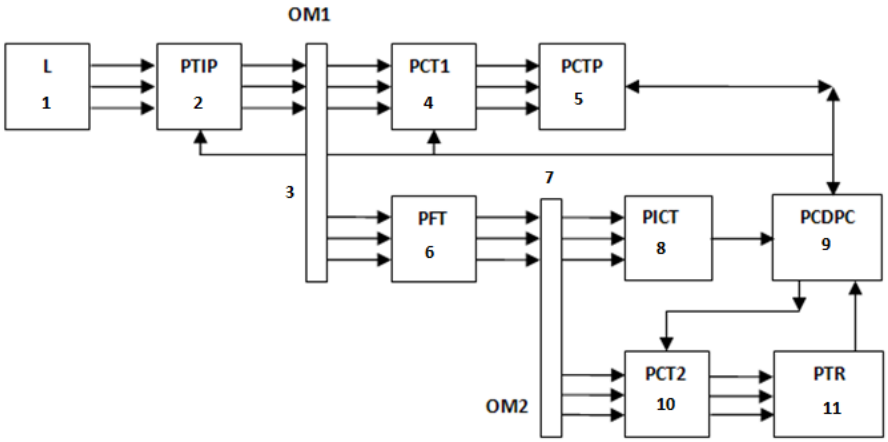

Figure 3. The structure of the system TRS4.

The system act in the next mode. 2-D image of the target P'(x',y') is input into the processor PTIP were are realized the operations of enhancement:

$$P'(x',y') \longrightarrow P(x',y') = P(x,y,e_1,e_2,e_3,e_4). \tag{18}$$

The optical beam formed by laser L going via processor PTIP is encrypted by the image P(x',y') after which is introduced via multiplier OM1 in the processors PCT1 and PFT. In the processor PFT, the Fourier spectrum of the target's image is formed:

$$P(x',y') = P(x,y,e_1,e_2,e_3,e_4) \longrightarrow |FT\{P(x',y')\}|^2=P(x'_1,y'_1) = P(x_1,y_1,e_1,e_2). \tag{19}$$

The P(x',y') image's parameters f_m and SL are determined in this unit. The function $P(x'_1,y'_1)$ is transmitted from processor PFT via multiplier OM2 to the processors PICT and PCT2. In the processor PICT, the chords transformation is calculated [13]:

$$P(x'_1,y'_1)\rightarrow P(x'_2,y'_2), \quad (20)$$

and the target's vector **v** of feature is calculated. The information regarding vector **v** is transferred from processor PICT to processor PCDPC, where the target is classified [16]. Also, in this processor, the target's scale e_1 is determined as $e_1=f_{ms}/f_m$, where f_{ms} is the Fourier spectrum's maximum frequency of the determined reference target. In the processor PCT2, the function $P(x'_1,y'_1)$ will be normalized on scale e_1 and converted to a polar coordinate system:

$$P(x'_1, y'_1)=P(x_1, y_1, e_1, e_2)\rightarrow P(x'_3,y'_3)=P[x_3 +x_{30}(e_2),y_3], \quad (21)$$

where $x_3=\text{arctg}(y''_1/x''_1)$, $y_3=[(x''_1)^2+(y''_1)^2]^{1/2}$ and $x''_1=x_1$, $y''_1=y_1/e_1$.

The function $P(x'_3,y'_3)$ is transferred from processor PCT2 to processor PTR, where the target's rotation e_2 is calculated based on the value $x_{30}(e_2)$ extracted. The data regarding parameters e_1 and e_2 are transmitted from unit PCDPC to unit PCT1, where the target's function P(x',y') is normalized on these parameters:

$$P(x',y') = P(x+e_3, y+e_4, e_1, e_2) \longrightarrow P(x'_4, y'_4) =P(x_4+e_3, y_4+e_4), \quad (22)$$

where $x'_4=[x'\cos(-e_2) - y\sin(-e_2)]/e_1$, $y'_4=[x'\sin(-e_2) + y\cos(-e_2)]/e_1$.

The function $P(x'_4, y'_4)$ is sent from processor PCT1 to processor PCTP, where the parameters e_3 and e_4 are determined based on the correlation function calculated between the function $P(x'_4,y'_4)$ and reference target's function $P_s(x_4,y_4)$ established on the stage of classification:

$$U(x_5,y_5) = \max\{\iint P(x'_4,y'_4)P_s(x_4,y_4)dx_4dy_4. \quad (23)$$

6. Models of data processing flow in the systems

The models of data processing flow in the systems which will be described in this section will permit the analysis of the efficiency of the computing processes organization in the systems and to optimize the systems' structures with the purpose of the increase their productivity.

6.1. Model of data processing flow in the system TRS1

Taking into account the system TRS1 operation presented in section 2, we will describe the stages of data processing in this system as follow. Stage S1/2 – target's image input and preprocessing in the processor 2; S2/4 – the target position in-plane (coordinates e_3, e_4) calculation in the processing unit 4; S2/9 - the Fourier spectrum of the target's image formation in processor 9, the maximum frequency f_m of the Fourier spectrum $P(x'_1,y'_1)$ and the complexity SL of image P(x',y') determination; S3/5 - the function P(x',y') centering in the processing unit 5 using the data regarding e_3, e_4, and SL; S4/7 - the operation of chord transformation performing in the processor 7 and the target's vector **v** of features calculation; S5/8 - the target classification in the processor 8; S6/8 - the target's scale e_1 determination in the processor 8; S7/10 - the target's image $P(x'_2,y'_2)$ normalization on e_1 and conversion to a polar coordinate system in the processor 10; S8/11 - the target's rotation (parameter e_2) calculation in the processing unit 11. The model MD1 of data processing flow is presented in Figure 4a.

6.2. Model of data processing flow in the system TRS2

Let's describe the stages of data processing in the system TRS2 in the next mode. Stage S1/2 – target's image input and preprocessing in the processor 2; S2/4 – the target position in-plane (coordinates e_3, e_4) calculation in the processing unit 4; S2/9 - the Fourier spectrum of the target's image formation in processor 9, the function P(x',y') complexity SL determination; S3/5 - the target's image centering (function P(x',y')) in the processing unit 5 using the data of e_3, e_4, and SL; S4/7 - the operation of chord transformation performing in the processor 7 and the target's vector **v** of features calculation; S5/8 - the target classification in the processor 8; S6/10 - the target's image (function $P(x'_2,y'_2)$) conversion to a log-polar coordinate system in the processor 10; S7/11 - the target's scale e_1 and rotation e_2 determination in the processor 11. The model MD2 of data processing flow in this system is presented in Figure 4b.

6.3. Model of data processing flow in the system TRS3

Let's determine the stages of data processing in the system TRS3, based on the system's description from section 4. Stage S1/2 – target's image input and preprocessing in processor 2; S2/4 – the target position in-plane (coordinates e_3, e_4) calculation in processor 4; S2/7 - the Fourier spectrum of the target's image formation in processor 7, the complexity

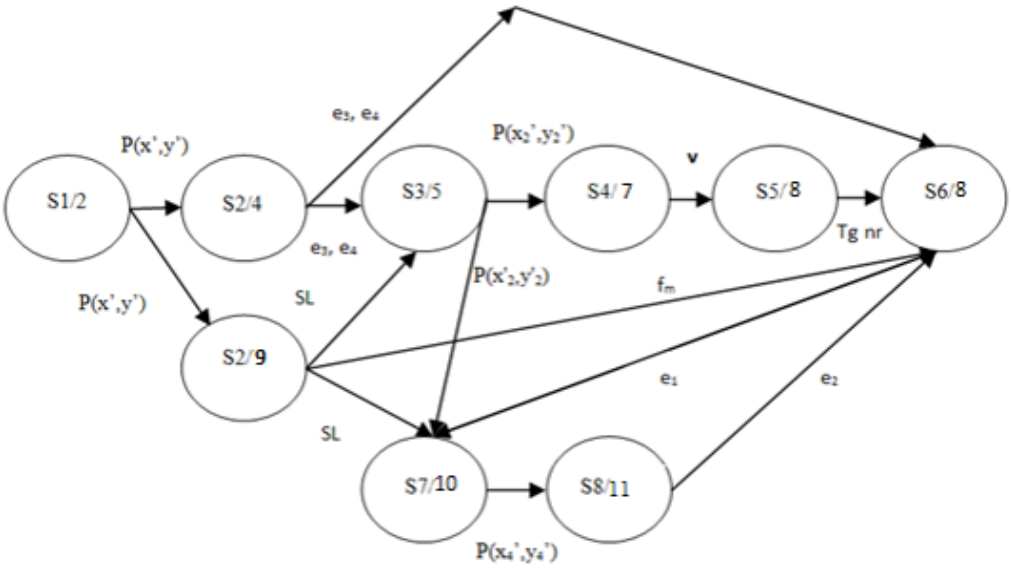

a)

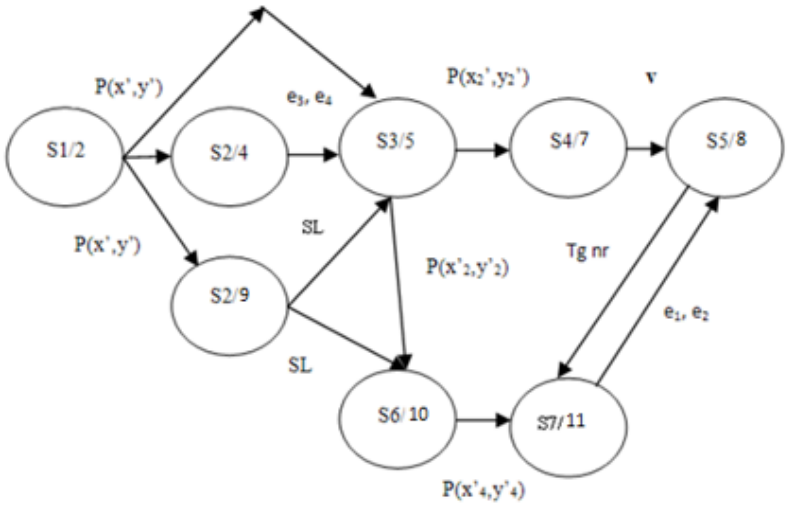

b)

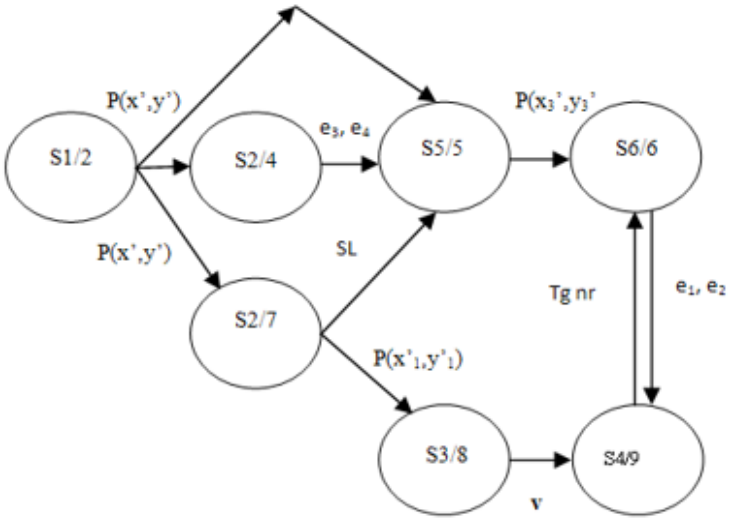

c)

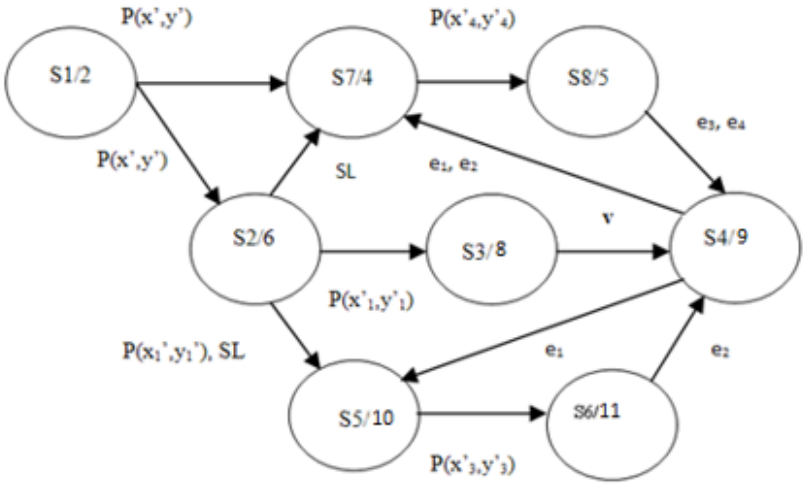

d)

Figure 4. The models of data processing flow in the systems: a) TRS1; b) TRS2; c) TRS3; d) TRS4.

SL of function P(x',y') calculation; S3/8 - the operation of chord transformation performing in the processor 8 and a feature vector **v** of the target calculation; S4/9 - the target classification in the processor 9; S5/5 - the target's image (function P(x',y')) normalization on parameters e_1 and e_2 in the processor 5 and conversion to a log-polar coordinate system; S6/6 - the target's scale e_1 and rotation e_2 determination in the processor 6. The model MD3 of data processing flow in the system is presented in Figure 4 c.

6.4. Model of data processing flow in the system TRS4

The stages of data processing in TRS4 can be formulated taking into account the respective functioning description (section 5), as follow. Stage S1/2 – target's image input and preprocessing in processor 2; S2/6 - the Fourier spectrum of the target's image formation in processor 6, the maximum frequency f_m and the complexity SL of image P(x',y') determination; S3/8 - the operation of chord transformation performing in the processor 8 and a vector **v** of the target's features calculation; S4/9 - the target classification in the processor 9 and determination of the target's scale e_1; S5/10 - the target's image spectrum (function $P(x'_1, y'_1)$) normalization on scale e_1 in the processor 10 and transformation to a polar coordinate system; S6/11 - the target's angular position e_2 calculation in the processing

unit 10; S7/4 – target's image normalization on parameters e_1 and e_2 in the processor 11; S8/5 – the target position in-plane (coordinates e_3, e_4) calculation in the processing unit 5. The model MD4 of data processing flow in this system is presented in Figure 4d.

7. Estimation of systems' data processing time and throughput

7.1. Determination of the processing time of the operations, realized in the systems

Let's determine the processing time of the operations, realized in the systems as follows. t_{PP} – the time of the target's image input and preprocessing, t_{PP} =6.6μs [9]; t_F – the total time of the operations: Fourier transform, and parameters f_m and SL calculation, t_F =4.24μs [14]; t_P - the time of the target's position in plane determination (parameters e_3, e_4), t_P =1.01μs [10]; t_{CT} – the time of the chord transformation of the centered target's image, t_{CT} =0.2μs [13]; t_{CT1} – the time of the chord transformation of the target's image Fourier spectrum, t_{CT}=t_{CT1}=0.2μs; t_S – the time of the target's scale e_1 calculation, t_S =0.04μs [11]; t_R – the time of the target's rotation e_2 calculation, t_R =53.7ms [15]; t_{SR} - the time of the target's scale e_1 and rotation e_2 determination in one step, t_{SR}=5.1+5.15N, μs [11]; t_C – the time of the target classification, t_C =(m_k -1)[DP(t_y+t_a)], where m_k is the number of the classes' targets; DP is the length of the target's image feature vector **v**; t_y, t_a - the multiplication and adding time, respectively [16]; t_{N0} – the time of the target's image normalization (centering) on values e_3, e_4; t_{N1} - the time of the target's image normalization on e_1 and transformation to a polar coordinate system; t_{N2} – the time of the target's image transformation to the log-polar coordinate system; t_{N3} – the time of the target's image normalization (centering) on parameters e_3, e_4 via Fourier spectrum calculation, t_{N3}=t_F=4.24μs; t_{N4} - the time of the target's image normalization (centering) on parameters e_3, e_4 and transformation to a log-polar coordinate system; t_{N5} - the time of the target's image spectrum normalization on e_1 and transformation to a polar coordinate system, t_{N5}=t_{N1}; t_{N6} - the time of the target's image normalization on data of e_1, e_2.

The values of parameters t_{N0} - t_{N6} can be determined as [12]: t_{Ni} = 14.2+α^2 N^2(t_{ep}+βt_{tpi}), where i=0÷6; the parameter α determine the complexity of the target's image; N – the total number of the target's image pixels in a row (colon); β – characterize the share of most informative pixels in the image; t_{ep} - time of the pixel's extracting from the target's image; t_{tpi} - time of the pixel's coordinates transformation. The data of parameters t_{tpi} will depend on the operation's kind realized, as follows: t_{tp0}=2t_a, t_{tp1}=t_{tp5}=t_a+4t_y+2t_f, t_{tp2}=t_a+3t_y+2t_f, t_{tp4}=3t_a+4t_y+2t_f, and t_{tp6}=2t_a+6t_y+2t_f, where t_a, t_y, and t_f are the times of adding, multiplication, and function calculation, respectively. The estimation of the data processing time and throughput of the systems was made for next values of the parameters: N=256, DP=180, m_k=10, α=0.5, β=0.1, G=NxN, t_{ep}=0.015μs, t_a=0.02μs, t_y=0.04μs, t_f=0.05μs. At these data, t_{SR}=1.3ms, t_C =97.2μs, t_{N0} =325.5μs, t_{N1}=718.7μs, t_{N2}=653.2μs, t_{N4}=784.2μs, t_{N6}=882.6μs

7.2. Estimation of the data processing time and throughput of the system TRS1

The system TRS1 data processing time will be determined in accordance with its functioning algorithm described in sections 2 and 6.1: T_{S1}=$t_{S1/2}$+max{$t_{S2/4}$,$t_{S2/9}$}+$t_{S3/5}$ +$t_{S4/7}$+$t_{S5/8}$+$t_{S6/8}$+$t_{S7/10}$+$t_{S8/11}$, were $t_{Si/j}$ is the time of the data processing on stage i in the processor j. The values of $t_{Si/j}$ will be determined as follows (section 7.1): $t_{S1/2}$=t_{PP}=6.6μs, $t_{S2/4}$=t_P=1.01μs, $t_{S2/9}$=t_F=4.24μs, $t_{S3/5}$=t_{N0}=325.5μs, $t_{S4/7}$=t_{CT}=0.2μs, $t_{S5/8}$=t_C=97.2μs, $t_{S6/8}$=t_S=0.04μs, $t_{S7/10}$= t_{N1}=718.7μs, $t_{S8/11}$=t_R=53.7ms. Taking into account that $t_{S2/8}$>$t_{S2/4}$,

$$T_{S1}=t_{S1/2}+t_{S2/9}+t_{S3/5}+t_{S4/7}+t_{S5/8}+t_{S6/8}+t_{S7/10}+t_{S8/11}=54.85\text{ms}. \quad (24)$$

The throughput of the system TRS1 will be $TP_{S1}=TIC/max\{t_{Si/j}\}$, where TIC is the target's image capacity. At TIC=256x256x8=524288 bits and $max\{t_{Si/j}\}=t_{S8/11}=53.7ms$, the processing time $TP_{S1}=9.7x10^6$ bits/sec. Figure 5 a. show, that the processing time on stage S8/11 is much bigger than on other stages, and the system is not optimal from the throughput point of view.

Obtaining an optimal system can be made by reducing the processing time on the stage S8/11 until the processing time on stages S7/10, at least, by changing the processors, implementing supplementary parallelism, etc. [17]. At the $t'_{S8/11}=t_{S7/10}$, the throughput of the modified system will increase up to $TP'_{S1}=729.5x10^6$ bits/sec, or, on $k_{S1}=TP'_{S1}/TP_{S1}=75$ times. The data processing time in the optimized system is estimated as:

$$T'_{S1}=t_{S1/2}+t_{S2/9}+t_{S3/5}+t_{S4/7}+t_{S5/8}+t_{S6/8}+2t_{S7/10}=1.87ms, \quad (25)$$

or, on $W_{S1}=T_{S1}/T'_{S1}=29.3$ times smaller than in the initial system.

7.3. Estimation of the data processing time and throughput of the system TRS2

The data processing time in the system TRS2 will be appreciated as: $T_{S2}=t_{S1/2}+max\{t_{S2/4},t_{S2/9}\}+t_{S3/5}+max\{\{t_{S4/7}+t_{S5/8}\},t_{S6/10}\}+t_{S7/11}$. The values of $t_{Si/j}$ will be estimated as (sections 6.2 and 7.1)): $t_{S1/2}=t_{PP}=6.6\mu s$, $t_{S2/4}=t_P=1.01\mu s$, $t_{S2/9}=t_F=4.24\mu s$, $t_{S3/5}=t_{N0}=325.5\mu s$, $t_{S4/7}=t_{CT}=0.2\mu s$, $t_{S5/8}=t_C=97.2\mu s$, $t_{S6/10}=t_{N2}=653.2\mu s$, $t_{S7/11}=t_{SR}=1.3ms$. Taking into account that $t_{S2/9}>t_{S2/4}$ and $t_{S6/10}>\{t_{S4/7}+t_{S5/8}\}$,

$$T_{S2}=t_{S1/2}+t_{S2/9}+t_{S3/5}+t_{S6/10}+t_{S7/11}=2.29ms. \quad (26)$$

The throughput of the system TRS2 will be evaluated as $TP_{S2}=TIC/max\{t_{Si/j}\}=403.3x10^6$ bits/sec. From Figure 5b is evident, that the processing time on stage S7/11 is much bigger than on other stages, and the system is not optimal.

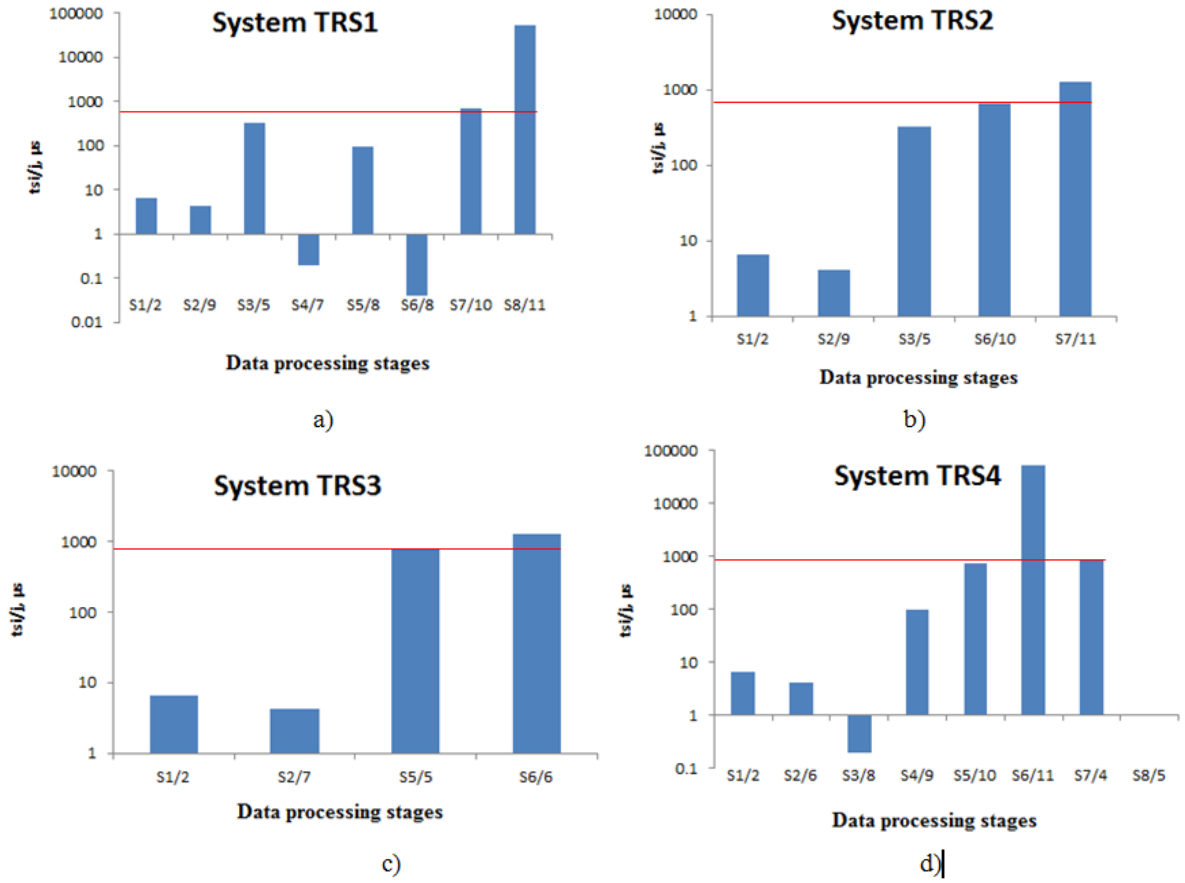

Figure 5. Processing time on different stages in the systems: a) TRS1; b) TRS2; c) TRS3; d) TRS4.

The enhancing of the system's characteristics is possible by reducing the processing time on stage S7/11 until the time on stage S6/10. At the $t'_{S7/11}=t_{S6/10}$, the throughput of the modified system will increase up to $TP'_{S2}=802.6x10^6$ bits/sec, or, on $k_{S2}=TP'_{S2}/TP_{S2}=2$ times. In this case, the data processing time will be:

$$T'_{S2}=t_{S1/2}+t_{S2/9}+t_{S3/5}+2t_{S6/10}=1.64ms, \quad (27)$$

or, on $W_{S2}=T_{S2}/T'_{S2}=1.4$ times less than in the initial system.

7.4. Estimation of the data processing time and throughput of the system TRS3

The data processing time in the system TRS3 can be determined as: $T_{S3}=t_{S1/2}+\max\{t_{S2/4},t_{S2/7}\}+\max\{\{t_{S3/8}+t_{S4/9}\}, t_{S5/5}\}+t_{S6/6}$.

The values of $t_{Si/j}$ will be estimated in the next mode: $t_{S1/2}=t_{PP}=6.6\mu s$, $t_{S2/4}=t_P=1.01\mu s$, $t_{S2/7}=t_F=4.24\mu s$, $t_{S3/8}=t_{CT}=0.2\mu s$, $t_{S4/9}=t_C=97.2\mu s$, $t_{S5/5}=t_{N4}=784.2\mu s$, $t_{S6/6}=t_{SR}=1.3ms$. Taking into account that $t_{S2/7}> t_{S2/4}$, and $t_{S5/5}>\{t_{S3/8}+t_{S4/9}\}$,

$$T_{S3}=t_{S1/2}+t_{S2/7}+ t_{S5/5}+t_{S6/6}=2.09ms. \quad (28)$$

The throughput of the system TRS3 will be evaluated as $TP_{S3}=TIC/\max\{t_{Si/j}\}=403.3x10^6$ bits/sec. From Figure 5c is evident, that the highest processing time in the system is on stage S6/6.

The optimization of the system is possible by reducing the processing time in this stage until stage S5/5. At the $t'_{S6/6}=t_{S5/5}$, the throughput of the modified system will increase up to $TP'_{S3}=668.5x10^6$bits/sec, or, on $k_{S3}=TP'_{S3}/TP_{S3}=1.66$ times. In this case, the processing time in the system will be:

$$T'_{S3}=t_{S1/2}+t_{S2/7}+2t_{S5/5}=1.58ms, \quad (29)$$

or, on $W_{S3}=T_{S3}/T'_{S3}=1.3$ times smaller than in the initial system.

7.5. Estimation of the data processing time and throughput of the system TRS4

The data processing time in the system TRS4 can be estimated as: $T_{S4}=t_{S1/2}+t_{S2/6}+t_{S3/8}+t_{S4/9}+t_{S5/10}+t_{S6/11}+t_{S7/4}+t_{S8/5}$.

The values of $t_{Si/j}$ will be determined as: $t_{S1/2}=t_{PP}=6.6\mu s$, $t_{S2/6}=t_F=4.24\mu s$, $t_{S3/8}=t_{CT}=0.2\mu s$, $t_{S4/9}=t_C=97.2\mu s$, $t_{S5/10}=t_{N5}=718.7\mu s$, $t_{S6/11}=t_R=53.7ms$, $t_{S7/4}= t_{N6}=882.6\mu s$, $t_{S8/5}=t_P=1.01\mu s$. For these data,

$$T_{S4}=t_{S1/2}+t_{S2/6}+t_{S3/8}+t_{S4/9}+t_{S5/10}+t_{S6/11}+ t_{S7/4}+t_{S8/5}=55.41ms. \quad (30)$$

The throughput of the system TRS4 will be estimated as $TP_{S4}=TIC/\max\{t_{Si/j}\}=9.7x10^6$ bits/sec. From Figure 5d is possible to conclude that the bigger processing time is on stage S6/11. The system throughput increasing is possible by reducing the processing time on this stage until stage S7/4.

At the $t'_{S6/11}=t_{S7/4}$, the throughput of the modified system will increase up to $TP'_{S4}=594x10^6$ bits/sec, or, on $k_{S4}=TP'_{S4}/TP_{S4}=61.2$ times. The data processing time in the optimized system will be:

$$T'_{S4}=t_{S1/2}+t_{S2/6}+t_{S3/8}+t_{S4/9}+t_{S5/10}+2t_{S7/4}+t_{S8/5}=2.59ms, \quad (31)$$

or, on $W_{S4}=T_{S4}/T'_{S4}=21.4$ times smaller than in the initial system.

7.6. Comparative analysis of the data processing time and throughput of the systems

The data regarding processing time and throughput of the elaborated initial and optimized systems are presented in Table 1 and Figures 6a, 6c and show the following.

The initial system TRS3 is characterized by a minimal processing time, T_{S3}=2.09ms. The processing time in the system TRS2 is small bigger, T_{S2}=2.29ms, or, in 1.1 times (Figure 6b). This time is much bigger in the system TRS1, T_{S1}=54,9ms (26.3 times), and in the system TRS4, T_{S4}=55.4ms (26.5 times).

Respectively, the throughput of the systems TRS2 and TRS3 is higher 41.5 times than that of the systems TRS1 and TRS4 (Figure 6d).

Table 1

The data of the initial and optimized systems

	TRS1	TRS2	TRS3	TRS4	TRS1´	TRS2´	TRS3´	TRS4´
Processing Time T_s, ms	54,9	2,29	2,09	55,41	1,87	1,64	1,58	2,59
Throughput TP_s, Mbs	9,7	403,3	403,3	9,7	729,5	802,6	668,5	594,0
$W_s=T_s/T'_s$	29,3	1,4	1,3	21,4				
$K_s=TP'_s/TP_S$					75,0	2,0	1,7	61,2

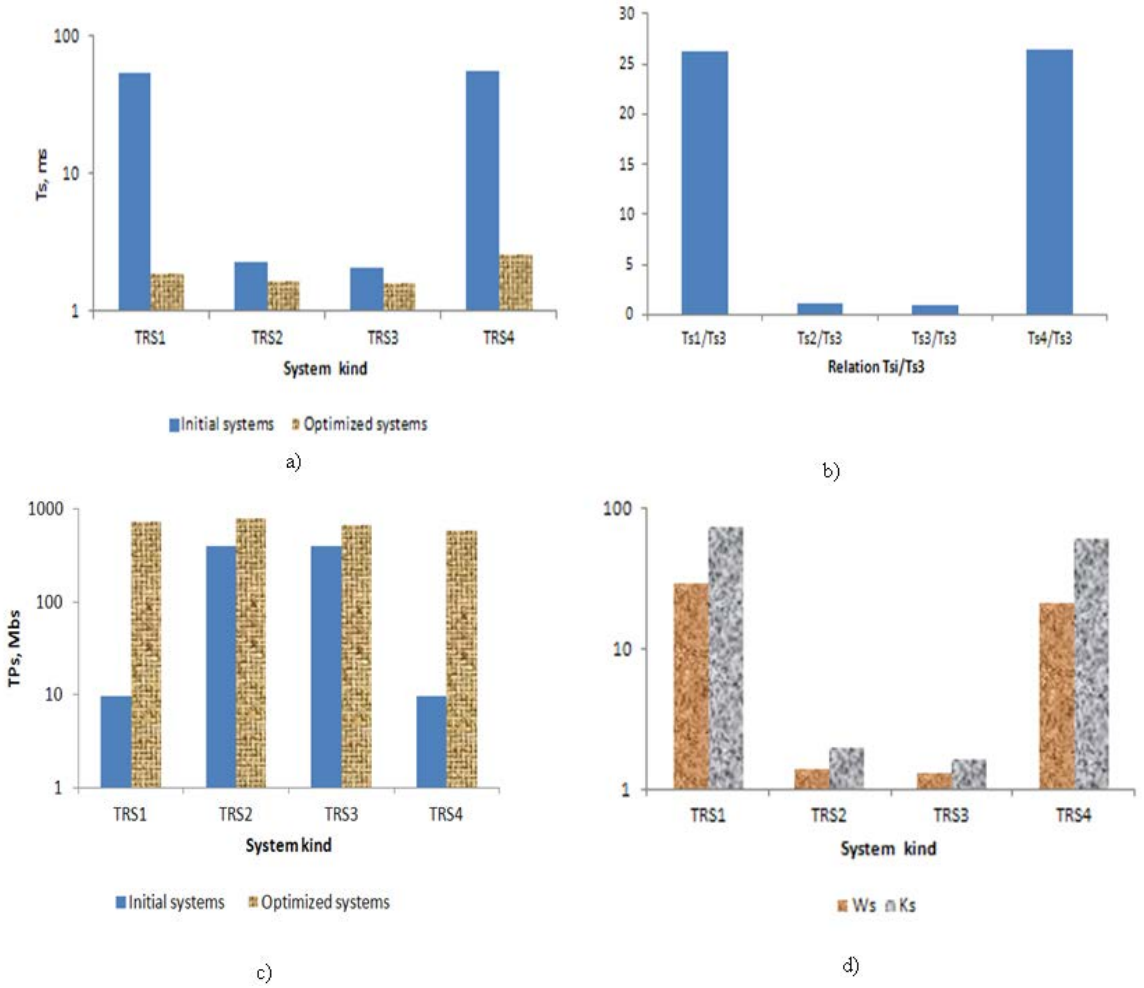

Figure 6. The data of the initial and optimized systems: a) – processing time; b) - relation T_{Si}/T_{S3}; c) – throughput; d) - effectiveness of the optimized systems in time – W_s, and productivity - K_s in comparison with initial systems.

Optimization permitted to decrease the processing time in the systems from 1.3 (system TRS3') until 29.3 times (system TRS1') and to increase the throughput of the systems from 1.7 (system TRS3') to 75 times (system TRS1').

The biggest optimization effect is referred to in the systems TRS3' and TRS4'. These systems are characterized by the very close processing time and throughput and can be effectively used in target recognition.

Conclusions

There were elaborated the structures of the four new specialized multiprocessor functional distributed systems, destinated for targets recognition and calculation of their position, scale, and rotation. The systems represent a combination of electronic and optical processing modules. The principles of their functioning are described.

The graphical models of data processing flow in the proposed systems are designed. The calculation of the processing time of the different operations, realized in the systems was made. The estimation of the data processing time and throughput of the systems' was done, based on the results of which the optimization of the proposed systems was made.

A comparative analysis of the data processing time and throughput of the systems was made which shows the following. The system TRS3 is characterized by a minimal processing time, T_{S3}=2.09ms. The processing time in the system TRS2 is small bigger, T_{S2}=2.29ms, or, 1.1 times. This time is much bigger in the system TRS1, T_{S1}=54,9ms (26.3 times), and in the system TRS4, T_{S4}=55.4ms (26.5 times). Respectively, the throughput of the systems TRS2 and TRS3 is higher 41.5 times than that of the systems TRS1 and TRS4.

Optimization permitted to decrease the processing time in the systems from 1.3 (TRS3') to 29.3 times (TRS1') and to increase the throughput of the systems from 1.7 (TRS3') to 75 times (TRS1'). The biggest optimization effect is obtained in the systems TRS3' and TRS4'. These systems are characterized by the very close processing time and throughput and can be effectively used in target recognition.

References

1. Haley J., Tucker J., Kessler B., Fish T. Bridging the gap from academia to application: rapid algorithm design and deployment for artificial intelligence (RADD-AI). Proc. SPIE 11870, Artificial Intelligence and Machine Learning in Defense Applications III, 118700A, 2021. DOI: 10.1117/12.2601858
2. Xie W., Ide J., Izadi D. at all. Multi-object tracking with deep learning ensemble for unmanned aerial system applications. Proc. SPIE 11870, Artificial Intelligence and Machine Learning in Defense Applications III, 118700I, 2021. DOI: 10.1117/12.2600209
3. Mediavilla C., Nans L., Marez D., Parameswaran S. Detecting aerial objects: drones, birds, and helicopters. Proc. SPIE 11870, Artificial Intelligence and Machine Learning in Defense Applications III, 118700J, 2021. DOI: 10.1117/12.2600068
4. Hollander R., Rooij S., Broek S. et all. Vessel classification for naval operations. Proc. SPIE 11870, Artificial Intelligence and Machine Learning in Defense Applications III, 118700N, 2021. DOI: 10.1117/12.2599513
5. Dominicis L., Bouma H., Toivonen S. et all. Video-based fusion of multiple detectors to counter-terrorism. Proc. SPIE 11869, Counterterrorism, Crime Fighting, Forensics, and Surveillance Technologies V, 118690J, 2021. DOI: 10.1117/12.2598147.
6. Kechagias-Stamatis O., Aouf N. Automatic Target Recognition on Synthetic Aperture Radar Imagery: A Survey. Computer Vision and Pattern Recognition, Dec 2020, pp.1-21. https://arxiv.org/abs/2007.02106.
7. Shu C., Sun L. Automatic target recognition method for multi-temporal remote sensing image. Open Physics, 2020, Volume 18 Issue 1, pp.170-181. https://doi.org/10.1515/phys-2020-0015.
8. Perju V. Methods of target recognition based on central image chord transformation. Journal of Engineering Science Vol. XXVIII, no. 4 (2021), pp. 52 - 62. ISSN 2587-3474/ eISSN 2587-3482. . https://doi.org/10.52326/jes.utm.2021.28(4).05.

9. Perju V., Casasent D. Optical-electronic multiprocessors computer systems controlled by input images parameters. In Optical Pattern Recognition XVI. David P. Casasent, Tien-Hsin Chao, Editors. Proc. SPIE 5816, pp. 306-314 (2005).
10. Perju V., Saranciuc D. et all. The operative analysis of the correlation fields in the optical processors. //Proc. of International Conference on Microelectronics and Computer Science ICMCS-97, 1997, Vol.2, pp.192-196, Chisinau, Republic of Moldova.
11. Perju V., Casasent D. Optical multichannel correlators for high-speed targets detection, recognition, and localization. In: Proc. SPIE 8398, 2012.
12. Perju V. The method of adaptive image coordinate transformation. In: Proc. SPIE 1978, pp. 280-288, 1993.
13. Perju V., Cojuhari V. Central and logarithmic central image chord transformations for invariant object recognition. In: Journal of Engineering Science. 2021, Vol. XXVIII, no. 1 (2021), pp. 38 - 46 ISSN 2587-3474/E-ISSN 2587-3482. https://doi.org/10.52326/jes.utm.2021.28(1).03.
14. Perju V., Casasent D. The investigation of the Fourier spectrum-based image complexity metrics for recognition applications. In: Proc. SPIE 8398, 2012. [21, JES]
15. Katys G., Perju V., Rotary S. *Methods and computer means of image processing*. Shtiintsa, Kishinev, 1991.
16. Perju V. Target recognition based on central and logarithmic central image chord transformations. Journal of Engineering Science. 2021, Vol. XXVIII, no. 2 (2021), pp. 44 – 52. ISSN 2587-3474/E-ISSN 2587-3482. https://doi.org/10.52326/jes.utm.2021.28(2).03
17. Perju V. Adaptive high-speed targets recognition systems controlled by the image's parameters. Proc. SPIE 11400, Pattern Recognition and Tracking XXXI, 114000S; 2020, DOI: 10.1117/12.2559616.